Silicon Naphthalocyanine Triplet State and Oxygen: A Reversible Energy-Transfer Reaction

Patricia A. Firey,[†] William E. Ford,[†,‡] James R. Sounik,[§] Malcolm E. Kenney,[§] and Michael A. J. Rodgers*[,†,‡]

Contribution from the Center for Fast Kinetics Research, University of Texas at Austin, Austin, Texas 78712, Center for Photochemical Sciences, Bowling Green State University, Bowling Green, Ohio 43403, and Department of Chemistry, Case Western Reserve University, Cleveland, Ohio 44106. *Received April 6, 1988*

Abstract: Naphthalocyanines are a new class of photodynamic sensitizers that strongly absorb far-red light. Energy transfer from the triplet (T_1) state of a silicon naphthalocyanine, bis(tri-*n*-hexylsiloxy)silicon 2,3-naphthalocyanine (SiNC), to ground-state $O_2(^3\Sigma_g^-)$ to produce singlet $O_2(^1\Delta_g)$ is shown by laser flash photolysis to be reversible in benzene and perdeuteriobenzene at 24 °C ($SiNC(T_1) + O_2(^3\Sigma_g^-) \rightleftharpoons SiNC(S_0) + O_2(^1\Delta_g)$). A model to account for the observed kinetics of this reaction is developed. The kinetic parameters obtained are independent of whether the equilibrium is approached by generating $SiNC(T_1)$ first (in the presence of $O_2(^3\Sigma_g^-)$) or by generating $O_2(^1\Delta_g)$ first (in the presence of $SiNC(S_0)$). The equilibrium constant K_{eq} determined is 0.014 ± 0.001, which corresponds to a standard free energy change of $\Delta G° = +2.5$ kcal/mol. Although energy transfer from $SiNC(T_1)$ to $O_2(^3\Sigma_g^-)$ is endergonic, the quantum yields of the SiNC triplet ($\Phi_T = 0.20 \pm 0.03$) and singlet O_2 ($\Phi_\Delta = 0.19 \pm 0.02$) are equal. Phosphorescence from SiNC in 2-methyltetrahydrofuran glass at 77 K indicates that the excited-state energy of $SiNC(T_1)$ is 21.5 kcal/mol, which is 1.0 kcal/mol below that of $O_2(^1\Delta_g)$.

In recent years the transfer of electronic energy to molecular oxygen from the triplet states of large molecules has become the concern of the biomedical community via the medium of photodynamic therapy of tumors. Singlet molecular oxygen, $O_2(^1\Delta_g)$, is regarded as a leading candidate for the initiation of tissue damage in the presence of light, oxygen, and an absorber. As tissue allows deeper light penetration with increasing wavelength in the range 600–1200 nm, the search for effective photodynamic sensitizers with high extinction coefficients in the deep red has been undertaken. In this laboratory we have focused on the naphthalocyanine class of tetrapyrroles, which typically absorb very strongly near 800 nm. While clinically desirable, such deep red absorbances also raise interesting photochemical questions. With such low excited singlet-state (S_1) energies and assuming reasonable singlet–triplet splittings, the triplet energy levels of such molecules might be close to, or even below, the energy level of singlet oxygen (22.5 kcal/mol).

Few molecules are known that have triplet-state energies close to that of singlet oxygen. β-Carotene, a potent quencher of singlet oxygen, has an energy level between 21 and 25 kcal/mol.[1] The triplet states of biliverdin and its dimethyl ester, with energies of approximately 21.5 kcal/mol, are close to that of the naphthalocyanine examined below, but they are not observably quenched by ground-state oxygen ($k_q < 10^8$ M^{-1} s^{-1}).[2] Few studies have been published on the photophysical properties of naphthalocyanines.[3-5] A recent study appeared on zinc(II) and aluminum(III) sulfonated naphthalocyanines, where the degree of sulfonation was indeterminate.[5] These derivatives were water-soluble but showed intense aggregation even at 10^{-6} M in aqueous media, and they were unstable toward photodecomposition. Preliminary studies by two of us[6] with a silicon naphthalocyanine derivative, bis(tri-*n*-hexylsiloxy)silicon 2,3-naphthalocyanine (SiNC) showed that this molecule was unusual with respect to its photophysical interactions with oxygen, and we suggested that the reaction between SiNC and singlet oxygen might be reversible. We have followed up these preliminary observations and here present a detailed account of the interaction of $SiNC(T_1)$ with oxygen.

Materials and Methods

SiNC was synthesized as described previously.[7] Hematoporphyrin IX dimethyl ester (HPDME) and protoporphyrin IX dimethyl ester (PPDME) were from Porphyrin Products. Zinc *meso*-tetraphenylporphyrin (ZnTPP) was from Aldrich, and metal-free *meso*-tetraphenylporphyrin (H_2TPP) was from Strem. Benzophenone was recrystallized from ethanol. The solvents used were benzene (spectroscopic grade, Fisher Scientific) and perdeuteriobenzene (Norell Inc.). 2-Methyltetrahydrofuran (2-MTHF) was distilled over $LiAlH_4$ to remove antioxidants.

Flash photolysis experiments were performed with a Q-switched Nd:YAG laser, which was either doubled or tripled in frequency to give single 10-ns light pulses at 355 or 532 nm. The third harmonic at 355 nm was used whenever direct excitation of SiNC was to be accomplished. This is in the region of the Soret band ($\epsilon \approx 90000$ M^{-1} cm^{-1}) for naphthalocyanines. The generated transient species were monitored at right angles to the laser beam in either 10 mm × 10 mm or 5 mm × 10 mm cells situated in a computer-controlled, single-beam kinetic spectrometer with nanosecond time resolution. Kinetic analyses were carried out with iterative least-squares fitting procedures.[8] Singlet oxygen luminescence (1.27 μm) was measured with a germanium photodiodide-based system having a time resolution of ≈600 ns.[9] Samples were held at constant oxygen concentrations by bubbling with mixtures of oxygen and nitrogen. The oxygen concentrations were calculated with 2.2 mM as the solubility of oxygen in air-saturated benzene.[10]

Triplet–triplet extinction coefficients ($\Delta\epsilon_T$) of SiNC in benzene were determined by the energy-transfer method.[11,12] Protoporphyrin IX dimethyl ester ($\Delta\epsilon_T = 30500$ M^{-1} cm^{-1} at 450 nm[13]), H_2TPP ($\Delta\epsilon_T = 50000$ M^{-1} cm^{-1} at 450 nm[14]), and ZnTPP ($\Delta\epsilon_T = 73000$ M^{-1} cm^{-1} at 475 nm[15]) were used as standards. Excitation was at 532 nm, where the extinction coefficient of the ground state of SiNC is relatively low ($\epsilon < 1000$ M^{-1} cm^{-1}). Laser intensities were attenuated so that the donor T_1 decay in the absence of naphthalocyanine was exponential.

Triplet quantum yields (Φ_T) of SiNC and singlet oxygen quantum yields (Φ_Δ) were made via the comparative method with excitation at 355

[†] University of Texas at Austin.
[‡] Bowling Green State University.
[§] Case Western Reserve University.

(1) Herkstroeter, W. G. *J. Am. Chem. Soc.* **1975**, *97*, 4161–4167.
(2) Land, E. J. *Photochem. Photobiol.* **1979**, *29*, 483–487.
(3) Darwent, J. R.; McCubbin, I.; Porter, G. *J. Chem. Soc., Faraday Trans. 2* **1982**, *78*, 903–910.
(4) Pyatosin, V. E.; Sevchenko, A. N.; Tsvirko, M. P. *Izv. Akad. Nauk SSSR, Ser. Fiz.* **1978**, *42*, 588–592.
(5) McCubbin, I.; Phillips, D. *J. Photochem.* **1986**, *34*, 187–195.
(6) Firey, P. A.; Rodgers, M. A. J. *Photochem. Photobiol.* **1987**, *45*, 535–538.
(7) Wheeler, B. L.; Nagasubramanian, G.; Bard, A. J.; Schechtman, L. A.; Dininny, D. R.; Kenney, M. E. *J. Am. Chem. Soc.* **1984**, *106*, 7404–7410.
(8) Foyt, D. C. *Comput. Chem.* **1981**, *5*, 49–54.
(9) Rodgers, M. A. J.; Snowden, P. T. *J. Am. Chem. Soc.* **1982**, *104*, 5541–5543.
(10) *Solubilities of Inorganic and Organic Compounds*; Stephen, H., Stephen, T., Eds.; Macmillan: New York, 1963; Vol. 1, p 573.
(11) Bensasson, R.; Land, E. J. *Trans. Faraday Soc.* **1971**, *67*, 1904–1915.
(12) Carmichael, I.; Hug, G. L. *J. Phys. Chem. Ref. Data* **1986**, *15*, 1–250.
(13) Sinclair, R. S.; Tait, D.; Truscott, T. G. *J. Chem. Soc., Faraday Trans. 1* **1980**, *76*, 417–425.
(14) Pekkarinen, L.; Linshitz, H. *J. Am. Chem. Soc.* **1960**, *82*, 2407–2411.
(15) Hurley, J. K.; Sinai, N.; Linschitz, H. *Photochem. Photobiol.* **1983**, *38*, 9–14.

0002-7863/88/1510-7626$01.50/0

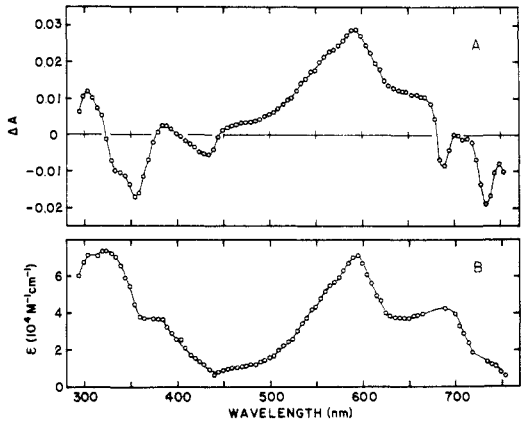

Figure 1. Difference and absolute triplet–triplet absorption spectra of SiNC in benzene. (a) Difference spectrum obtained 3 μs after 355-nm laser excitation of an N_2-saturated solution of SiNC (2.3 μM). The monochromator slit width was 1 mm. (b) Absolute spectrum obtained by adding the spectrum of ground-state SiNC in benzene (ϵ = 64 000 M^{-1} cm^{-1} at 690 nm) to the difference spectrum in a, where $\Delta\epsilon$ = 70 000 M^{-1} cm^{-1} at 590 nm.

nm. For the determination of Φ_T, the solvent was benzene (or perdeuteriobenzene), and benzophenone ($\Delta\epsilon_T$ = 7200 M^{-1} cm^{-1} at 532 nm, Φ_T = 1.0[15]) and ZnTPP ($\Delta\epsilon_T$ = 73 000 M^{-1} cm^{-1} at 475 nm, Φ_T = 0.83[15]) were used as standards. For the determination of Φ_Δ, the solvent used was perdeuteriobenzene (C_6D_6) in order to minimize the influence of the intense initial luminescence arising from SiNC fluorescence, thereby allowing a more precise extrapolation to t = 0. The standard used was benzophenone (Φ_Δ = 0.29[16]). In a separate experiment, it was determined that the Φ_Δ's of benzophenone in benzene and perdeuteriobenzene were equal.

The steady-state red-infrared luminescence of samples was measured with an apparatus that was constructed in-house on the basis of designs (with modifications) of Khan[17] and Kanofski.[18] It consisted of a 100-W Hg arc lamp with lens assembly (Oriel) or a large-frame Kr ion laser, which excited the sample held in a 10 mm × 10 mm cuvette. A beam chopper (Brower Laboratories Inc. Model 312C) was placed between the excitation source and the sample cuvette, as were lamp filters consisting of 10 cm of water, a KG3 heat filter, and a Hg-line filter where appropriate. For low-temperature work, the cuvette was held in a Dewar with two optical windows at right angles to each other. For room-temperature work, a spherical mirror placed behind the cuvette increased collected light. In all cases luminescence was monitored at right angles to the excitation. The emitted light was collected by a Cassegrain f/1 light collector. After it passed through cutoff and order-blocking filters, the light passed through a monochromator (PTI, computer controllable) with a grating of 600 L/mm, 1-μm blaze. The detector was a liquid-nitrogen-cooled germanium detector and preamplifier (Northcoast Scientific Corp. Model EO-817L). A Northcoast Muon filter (Model 829B) was used as an electronic signal filter, before the signal was sent to a lock-in amplifier (Princeton Applied Research Model 124A). The system was interfaced to a data station consisting of an XT-compatible personal computer and Hewlett Packard plotter. When actinometry coupled to measurements of standardized singlet oxygen systems was used, it was determined that the detection level for luminescence at 1.27 μm was ca. 1 mV/nmol of singlet oxygen. Background due to scattered light and amplifier noise was significantly less than 100 μV. The usable wavelength region covered ca. 700–1600 nm.

Results

Light-Induced Transient Absorptions in SiNC. Solutions of SiNC (2.3 μM) in benzene that were deaerated by bubbling with N_2 gas produced an absorbing species with λ_{max} between 590 and 595 nm when subjected to a 355-nm pulse (10 ns) of light (Figure 1a). Under low laser intensity this species decayed exponentially with a lifetime of ca. 330 μs, which was shortened in the presence of oxygen (see below). When porphyrins such as PPDME, ZnTPP, or H_2TPP were present (60–80 μM) in addition to SiNC (20–70 μM), and excitation was carried out at 532 nm, where

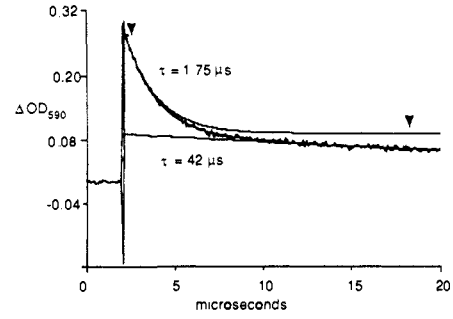

Figure 2. Time profile of the absorbance change at 590 nm following 355-nm laser excitation of an air-saturated solution of SiNC (12 μM) in benzene. A least-squares fit to two first-order decay components having lifetimes of 1.75 and 42 μs is superimposed on the experimental curve. Transient difference spectra obtained at the times indicated by arrows were the same.

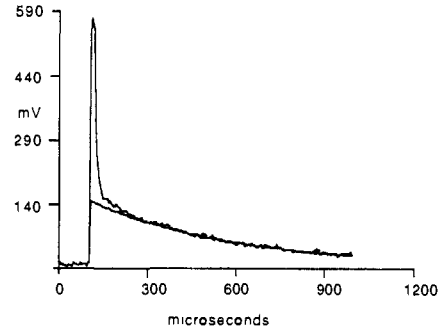

Figure 3. Time profile of infrared emission following 355-nm laser excitation of an air-saturated solution of SiNC (1.9 μM) in perdeuteriobenzene. A least-squares fit of the latter part of the curve to a first-order decay with a lifetime of 450 μs is superimposed on the experimental curve. The initial fast spike and associated shoulder is an artifact attributed, at least in part, to SiNC fluorescence.

SiNC had a negligible absorption; the porphyrin T_1 states (λ_{max} = 450–475 nm), which were produced initially, were observed to decay more rapidly than in the absence of SiNC. Concomitantly, the absorption band around 590 nm was formed. Taken together, these observations are consistent with the 590-nm band (Figure 1a), arising from the $T_1 \rightarrow T_n$ absorption of SiNC.

Quantitative experiments using the porphyrin sensitizers enabled a $\Delta\epsilon_T$ at 590 nm of 70 000 ± 8500 M^{-1} cm^{-1} in benzene to be evaluated. When this value of $\Delta\epsilon_T$ is used, the difference spectrum (Figure 1a) was corrected for bleaching of the ground state of SiNC in benzene (λ_{max} = 776 nm, $\epsilon = 5.4 \times 10^5$ M^{-1} cm^{-1}) to obtain the absolute absorption spectrum of the SiNC T_1 state. This is shown in Figure 1b. When benzophenone or ZnTPP was used as reference material, a value of Φ_T = 0.20 ± 0.03 was measured.

Under air-saturated conditions in benzene the decay rate of the 590-nm absorbance was enhanced and a departure from exponentiality was clearly observable (Figure 2). At the times indicated by the arrows in Figure 2, the spectral properties were identical, indicating that oxygen was not causing any changes in the nature of the absorbing species. This nonexponential behavior was maintained over a range of oxygen and SiNC concentrations. In all cases, the time-variable triplet concentration $[T_1]_t$ could be fitted by an expression of the general form given in eq 1. It

$$[T_1]_t = a_1 e^{-\gamma_1 t} + a_2 e^{-\gamma_2 t} \quad (1)$$

was found that the amplitudes of the preexponential factors a_1 and a_2 were dependent on both SiNC and O_2 concentrations.

Time-Resolved Infrared Luminescence Measurements. Air-saturated solutions of SiNC (2 μM) in benzene, when excited by 10-ns pulses of 355-nm light, emitted luminescence in the near infrared around 1.27 μm. Figure 3 shows a typical emission profile for a perdeuteriobenzene solution. The slow component is the emission from $O_2(^1\Delta_g)$ formed by energy transfer from SiNC(T_1) states. The early component is the decay of residual SiNC

(16) Gorman, A. A.; Hamblett, I.; Rodgers, M. A. J. *J. Am. Chem. Soc.* **1984**, *106*, 4679–4682.
(17) Khan, A. U. *Chem. Phys. Lett.* **1980**, *72*, 112–114.
(18) Kanofsky, J. R. *J. Biol. Chem.* **1983**, *258*, 5991–5993.

fluorescence of $\lambda > 1100$ nm that is passed by the silicon cut-off filter (see below). Fitting the slow component with an exponential and extrapolating back to time zero provides a measure of the singlet oxygen signal amplitude prior to the onset of the decay. This is proportional to the number of singlet oxygen molecules formed in the energy-transfer step. Comparison of this value with that obtained when benzophenone in the same solvent was used as sensitizer under identical absorption and excitation conditions gave $\Phi_\Delta = 0.19 \pm 0.02$, which is the same as Φ_T. Thus, every oxygen-quenching interaction leads to $O_2(^1\Delta_g)$.

Reversible Energy Transfer. The rate of decay of the singlet oxygen luminescence signal from SiNC in C_6D_6 paralleled that of the decay of the slow component of the absorption of the T_1 state. Likewise, the decay rate of the early component of the T_1 state absorbance, as well as the amplitude of the preexponential factors, all showed dependence on SiNC and O_2 concentrations. These facts are consistent with reversible energy transfer between SiNC and oxygen. The following model is proposed

$$\begin{array}{ccc} N_T + \Sigma & \underset{k_r}{\overset{k_f}{\rightleftharpoons}} & N_G + \Delta \\ {\scriptstyle k_T}\downarrow & & \downarrow{\scriptstyle k_\Delta} \\ N_G & & \Sigma \end{array}$$

where N_G and N_T represent ground and T_1 states of the naphthalocyanine, Σ and Δ represent the $^3\Sigma_g^-$ and $^1\Delta_g$ states of molecular oxygen, and k_f, k_r, k_T, and k_Δ are the rate parameters coupling the four species. Under our experimental conditions the concentrations of Σ and N_G are always greater than those of Δ or N_T at any time; hence, the forward and reverse reactions in the equilibrium are kinetically first order. The resulting situation is analogous to the aromatic hydrocarbon excited monomer–excimer equilibrium, which has been comprehensively treated by Birks and his students.[19] The complete solution for the temporal decay of N_T is complicated but is of the same form as eq 1. However, at high temperatures, i.e., where the forward and reverse processes in the equilibrium are significantly faster than the equilibrium-draining rates (k_T and k_Δ), the analytical expressions become simpler and more useful. Thus

$$\gamma_1 = k_r[N_G] + k_f[\Sigma] \quad (2)$$

$$\gamma_2 = k_T(k_r[N_G]/(k_r[N_G] + k_f[\Sigma])) + k_\Delta(k_f[\Sigma]/(k_r[N_G] + k_f[\Sigma])) = X_T k_T + X_\Delta k_\Delta$$

where γ_1 and γ_2 are the measured rates of the early and late components of the triplet decay (see eq 1) and X_T and X_Δ are the mole fractions of the N_T and Δ species at equilibrium ($X_T = [N_T]/([N_T] + [\Delta])$ and $X_\Delta = [\Delta]/([N_T] + [\Delta])$).

To verify that eq 2 describes the system under consideration, we investigated the variance of γ_1 with SiNC and O_2 concentrations in a series of separate experiments. The results are shown in Figure 4. Clearly, the data are consistent with eq 2, and values of $k_r = 1.14 \times 10^{10}$ M^{-1} s^{-1} and $k_f = 1.6 \times 10^8$ M^{-1} s^{-1} were extracted. Thus, on the basis of forward and reverse rate constants, we found the equilibrium constant ($K_{eq} = k_f/k_r$) to be 0.014.

Alternatively, K_{eq} was obtained from the values of the SiNC(T_1) concentrations at $t = 0$ (A_0) and at equilibrium (A_∞). Since all quenching acts yield singlet oxygen

$$K_{eq} = ([N_G]/[\Sigma])[(A_0 - A_\infty)/A_\infty]$$

In this case, the A_0 and A_∞ values were obtained from the experimental curves such as in Figure 2. Values of K_{eq} obtained by this method with SiNC concentrations in the range 6–17 μM and O_2 concentrations in the range 0.5–10.5 mM yielded an average value of 0.014 ± 0.001. Thus, both the kinetic and equilibrium measurements gave $K_{eq} = 0.014 \pm 0.001$ at 24 °C.

Slow Component of the SiNC Triplet Decay. In the high-temperature limit of the kinetic model, the parameter γ_2 is independent of whether the process under consideration is that of the T_1 or $^1\Delta_g$ species, i.e., both species decay with a common rate parameter (γ_2), which is the decay rate of the equilibrium state. This was in fact observed when the solvent was C_6D_6.

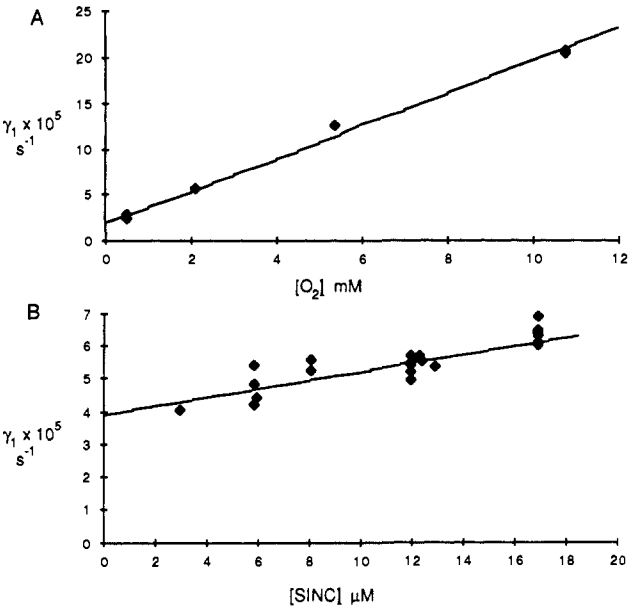

Figure 4. Plots of the rate constant for the early component (γ_1) of the SiNC triplet decay in benzene: (a) versus the concentration of O_2 (SiNC concentration 12 μM); (b) versus the concentration of SiNC (O_2 concentration 2.2 mM). Linear least-squares fits of the data to eq 2 are shown.

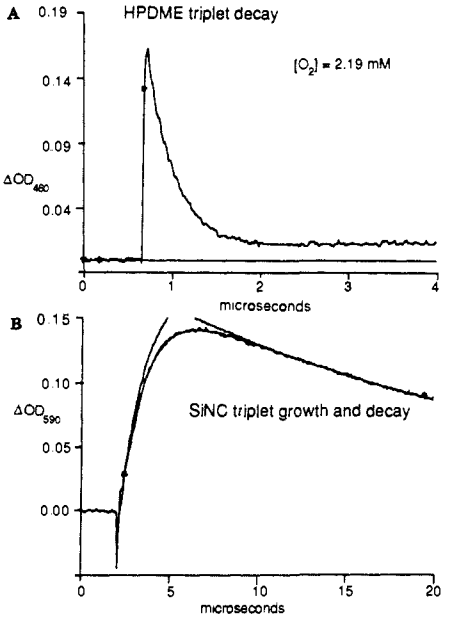

Figure 5. Time profiles of absorbance changes at (a) 460 nm and (b) 590 nm following 532-nm laser excitation of an air-saturated solution of 20 μM SiNC and 100 μM HPDME in benzene. Least-squares fits of the first-order decay in absorbance at 460 nm (due mainly to HPDME-(T_1)) and rise in absorbance at 590 nm (due mainly to SiNC(T_1)) are superimposed on the experimental curves.

Energy Transfer from $O_2(^1\Delta_g)$ to SiNC. The equilibrium constant of 0.014 indicates that the T_1 state of SiNC is favored over $O_2(^1\Delta_g)$ in oxygen-containing solutions. Thus, we should be able to approach the equilibrium position from the reverse direction. To show this, we prepared aerated benzene solutions of HPDME (10^{-4} M) in the presence and absence of SiNC (20 μM) and excited with 532-nm light pulses. At this wavelength under these conditions HPDME is the species that is absorbing virtually all the light. The T_1 state of HPDME, formed within a few tens of nanoseconds through intersystem crossing, absorbs at 490 nm. Under the experimental conditions, in the absence of SiNC, the

(19) Birks, J. B. *Photophysics of Aromatic Molecules*; Wiley: New York, 1970; pp 301–311.

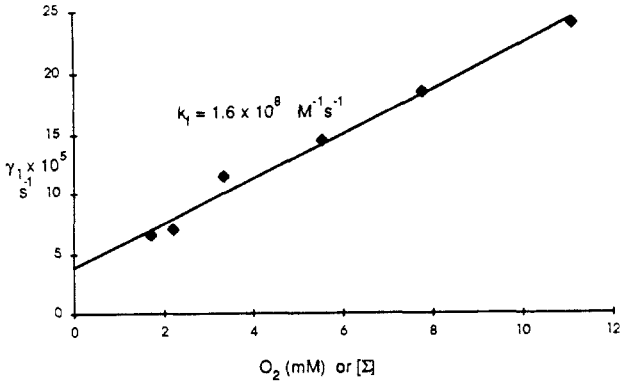

Figure 6. Plot of the pseudo-first-order rate constant for the rise in absorbance at 590 nm (due mainly to SiNC(T_1)) in the solution containing SiNC and HPDME (same as in Figure 5) versus the concentration of O_2. A linear least-squares fit of the data to eq 2 is also displayed.

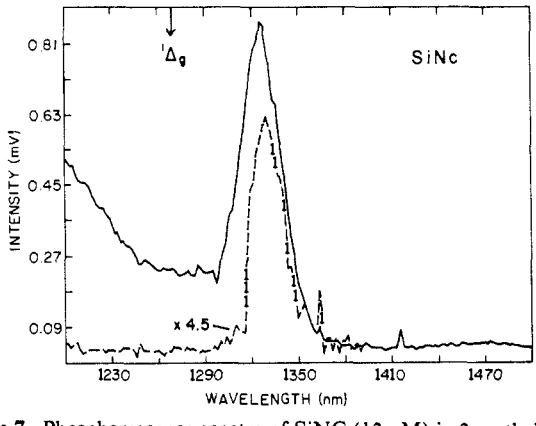

Figure 7. Phosphorescence spectra of SiNC (13 μM) in 2-methyltetrahydrofuran glass at 77 K obtained with monochromator slit widths of 3 mm (—) and 1 mm (---). The apparent emission below 1300 nm probably arises from spectral impurities. The excitation wavelength was 676 nm (Kr ion laser).

T_1 lifetime (due to oxygen quenching) was 0.26 μs (Figure 5a). This reaction is well-known to produce singlet oxygen with high efficiency.[20] In the presence of SINC, an absorbance that peaked at 590 nm grew with a lifetime of 1.3 μs (Figure 5b). This species subsequently decayed over several microseconds. The first-order rate constant of the growth at 590 nm (SiNC(T_1)) was linearly proportional to the oxygen concentration (Figure 6) with a slope of 1.6×10^8 M^{-1} s^{-1}. This corresponds to the same value of k_f as obtained from the oxygen quenching of SiNC(T_1) formed initially by 355-nm photon absorption. Sensitization of the T_1 state of SiNC by energy transfer directly from T_1 of HPDME ($k = 1.5 \times 10^9$ M^{-1} s^{-1}) was negligible under these conditions.

Infrared Luminescence Studies (Steady State). In an earlier preliminary communication from this laboratory,[6] it was noted that the fluorescence of SiNC in dilute solution in benzene extended from 790 to beyond 1400 nm. Further, in aerated solutions, a small but discernable spectral band with $\lambda_{max} = 1270$ nm was detected (arising from the weak $^1\Delta_g \rightarrow {}^3\Sigma_g^-$ transition in O_2). In deaerated solution this band disappeared, but a new band with $\lambda_{max} = 1330$ nm was seen. This band was absent with oxygen present and was attributed to a phosphorescence ($T_1 \rightarrow S_0$) transition in SiNC. To confirm and amplify this observation, we have conducted spectral studies of the red-infrared luminescence from SiNC in 2-MTHF glass at 77 K. The results are shown in Figure 7 where luminescence is seen with a strong band around 1330 nm. At room temperature with air present the 1330-nm peak was missing. The two spectra in Figure 7 show the effect of slit width on the luminescence signal. With slits in excess of 1 mm, a signal at wavelengths between 1200 and 1300 nm appears out of the background. Running this same experiment in oxygenated liquid solutions of red-light absorbers such as porphyrins, xanthenes, phthalocyanines, and naphthalocyanines at high slit widths (to optimize the weak 1.27-μm light from singlet oxygen) has consistently shown continuum emission in the 1200–1300-nm region not related to $O_2(^1\Delta_g)$. That, with the system here, this emission can be preferentially eliminated at narrow bandwidths implies that it arises from spectral impurities and not the long wavelength part of the fluorescence, as thought hitherto. We plan more detailed studies in this area.

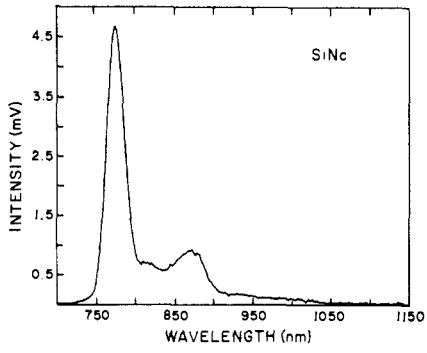

Figure 8. Fluorescence spectrum of SiNC (0.2 μM) in 2-methyltetrahydrofuran at 24 °C. The excitation wavelength was 676 nm (Kr ion laser), and the monochromator slit width was 2.5 mm. The spectrum was not corrected for the wavelength-dependent sensitivity of the germanium diode detector.

The fluorescence spectrum of a solution of SiNC in 2-MTHF at 24 °C over the range 700–1150 nm is shown in Figure 8. This spectrum was obtained under optically dilute conditions (A = 0.088/cm at the 774-nm absorption band maximum) and thus is an improved version of previously published work.[7]

Discussion

The evidence presented above lead us to conclude that the SiNC triplet state, produced in a 20% yield following photoexcitation, interacts with oxygen molecules in a reversible process. The energy-transfer studies lead to an equilibrium constant of 0.014, or $\Delta G°$ = 2.5 kcal/mol at 24 °C for energy transfer to O_2. Thus, the energy transfer to oxygen is slightly endergonic.

The spectroscopic studies allow further elaboration of this point. From the fluorescence spectrum (Figure 8) it is noted that the two highest energy peaks are at 776 and 815 nm. These correspond to the $S_1(v = 0)$ to the $S_0(v = 0)$ and $S_0(v = 1)$ transitions, respectively,[7] and the energy separation is ca. 620 cm^{-1}. This therefore is the spacing between the two lowest vibrational states of S_0 in SiNC. The 1330-nm phosphorescence band at 77 K (Figure 7) shows no structure and its half-width is not more than 30 nm or 170 cm^{-1}, which precludes its being an envelope of the total ground-state vibrational frequencies. Thus, the 1330-nm band corresponds to a transition from T_1 to a single vibrational level of S_0.

We cannot state unequivocally that the 1330-nm band arises from the $T_1(v = 0)$ to $S_0(v = 0)$ transition, although this is arguably the case. If the 0, 0 transition were not the 1330-nm band, then it would be at shorter wavelengths. However, we have been unable to detect any oxygen-dependent peaks at shorter wavelengths, though admittedly the more intense fluorescence in these regions would tend to make their observation difficult. On balance, we feel that the assignment of the phosphorescence band to the $T_1(v = 0)$ to $S_0(v = 0)$ transition is consistent with the evidence. Consequently, this leads to the conclusion that the T_1 state is 7520 cm^{-1} (1330 nm) above $S_0(v = 0)$, an energy gap of 21.5 kcal/mol.

The $O_2(^1\Delta_g) \rightarrow O_2(^3\Sigma_g)$ (0, 0) transition in oxygen is at 22.5 kcal/mol (1269 nm). Therefore, from spectroscopic measurements, energy transfer from the SiNC T_1 state to oxygen is endergonic by 1.0 kcal/mol. This is 40% of the gap indicated by the energy-transfer data, which, as reported above, is 2.5 kcal/mol. The 1.5 kcal/mol difference between the spectroscopic and

(20) Keene, J. P.; Kessel, D.; Land, E. J.; Redmond, R. W.; Truscott, T. G. *Photochem. Photobiol.* **1986**, *43*, 117–120.

equilibrium-derived triplet-state energies may be understood in terms of the spin statistical factor. Thus, in going from SiNC(T_1) to $O_2(^1\Delta_g)$ only one-ninth of the intervening collision complexes are of overall singlet multiplicity, whereas for the reverse process there are only uniquely singlet complexes. This effect results in the equilibrium-derived T_1 energy value being depressed from the spectroscopic value by a factor of $RT \ln (^1/_9) = 1.3$ kcal/mol at 24 °C. This brings the two values in line.

Conclusion

This work confirms our earlier preliminary conclusion that energy transfer from the triplet state of SiNC to O_2 to produce singlet oxygen is a reversible reaction. A kinetic model for the reaction satisfactorily accounts for the results of laser flash photolysis experiments and makes it possible to evaluate the rate and equilibrium constants. This model is supported by the fact that the kinetic parameters obtained are independent of whether the equilibrium is approached by generating SiNC(T_1) first (in the presence of $O_2(^3\Sigma_g^-)$) or by generating $O_2(^1\Delta_g)$ first (in the presence of SiNC(S_0)). Although energy transfer from SiNC(T_1) to $O_2(^3\Sigma_g^-)$ is endergonic, the efficiency of conversion of the triplets into singlet oxygen is nearly 100% because the SiNC triplet is intrinsically long-lived and the equilibrium state is drained mainly via the decay of $O_2(^1\Delta_g)$.

Acknowledgment. The laser flash photolysis and data analyses were carried out at the Center for Fast Kinetics Research at the University of Texas at Austin. The CFKR is supported jointly by NIH Grant RR 00886 from the Biotechnology Branch of the Division of Research Resources and by the University of Texas at Austin. Support for this project came from NIH Grant GM 24235. We thank Dr. A. A. Gorman for enlightening discussions.

Registry No. O_2, 7782-44-7; SiNC, 92396-88-8.

Photoelectrochemistry of Strained-Layer and Lattice-Matched Superlattice Electrodes: Effects Due to Buffer Layers

A. J. Nozik,* B. R. Thacker, J. A. Turner, and M. W. Peterson

Contribution from the Solar Energy Research Institute, Golden, Colorado 80401.
Received April 25, 1988

Abstract: Strained-layer and lattice-matched superlattice electrodes have been studied and compared as photoelectrodes in photoelectrochemical cells, and the effects of the presence of buffer layers in the strained-layer systems have been established. Photocurrent spectroscopy and photomodulated reflectance spectroscopy of superlattice electrodes, etched superlattice electrodes, and buffer layer structures reveal that highly strained superlattices (1.8% mismatch) have poorly defined quantization effects in their quantum wells; strained-layer superlattices with less mismatch (0.9%) have better defined quantization, but this is not reflected in their photocurrent spectra. On the other hand, lattice-matched superlattice electrodes exhibit extremely well-defined quantization effects that are clearly exhibited in multiple photocurrent peaks that match theoretical predictions; photomodulated reflectance spectra exhibit 17 transitions that represent all the possible allowed transitions in the quantum wells, including all light and heavy hole transitions, as well as unconfined transitions above the well barriers. The present work indicates that previous results reported for the photoelectrochemistry of highly strained superlattices probably reflected a photoresponse that was influenced more by the buffer layers than by the superlattice layers. The occurrence of hot electron transfer from photoexcited superlattice electrodes remains to be demonstrated unequivocally.

The photocurrent action spectra of superlattice electrodes in photoelectrocheical cells have been reported[1-3] to exhibit interesting features that have been attributed to the presence of discrete energy level structure in the quantum wells of the superlattice. Results with both lattice-matched superlattices (LMS), consisting of GaAs quantum wells and $Al_{0.38}Ga_{0.62}As$ barriers,[1] and strained-layer superlattices (SLS), consisting of GaAs wells and $GaAs_{0.5}P_{0.5}$ barriers,[2,3] have been described.

Because of the lattice mismatch between the GaAs and $GaAs_{0.5}P_{0.5}$ layers, strained-layer superlattices require a series of buffer layers between the single-crystal substrate and the superlattice that are graded in composition in order to provide a composition for the last buffer layer that is equal to the average composition of the superlattice layers; this is necessary to minimize misfit dislocations and produce good morphology in the superlattice.[4] Lattice-matched superlattices do not require such a series of buffer layers; the superlattice is simply grown on top of a single GaAs epilayer deposited on a GaAs single-crystal substrate.

In our previous study of SLS electrodes,[2,3] they consisted of a single-crystal p^+-GaAs substrate, a nondeliberately doped GaAs epilayer, five nondeliberately doped buffer layers, and a 20-period superlattice with 250-Å GaAs wells and either 250- and 40-Å $GaAs_{0.5}P_{0.5}$ barriers. We assumed that the observed photocurrent from these electrodes was generated only in the superlattice layers, and we completely neglected any contributions from the underlying $GaAs_{1-x}P_x$ buffer layers or from a possible p–n junction between the p^+-GaAs substrate and the undoped p-GaAs epilayer. This assumption would be valid for cathodic photocurrent in our particular sample configuration if the buffer layers are p-type, since under these conditions electrons must flow against a series of potential barriers created by the heterojunctions between the buffer layers. Although Mott–Schottky data for our SLS electrodes indicated p-type character over the potential regions where the photocurrent is cathodic, we have found recent experimental results that indicate the buffer layers behave n-type and contribute significant photocurrent at wavelengths above 775 nm. Furthermore, a fortuitous complication is that the band gaps of the five $GaAs_{1-x}P_x$ buffer layers in our samples overlap some of the theoretical energy transitions for the GaAs quantum wells in our superlattices. These quantum wells comprise a total thickness of 0.5 μ and absorb between 40 and 60% of the incident light between 850 and 700 nm, respetively; the rest of the light passes

(1) Nozik, A. J.; Thacker, B. R.; Turner, J. A.; Klem, J.; Morkoc, H. *Appl. Phys. Lett.* **1987**, *50*, 34.
(2) Nozik, A. J.; Thacker, B. R.; Turner, J. A.; Olson, J. M. *J. Am. Chem. Soc.* **1985**, *107*, 7805.
(3) Nozik, A. J.; Thacker, B. R.; Olson, J. M. *Nature (London)* **1985**, *316*, 6023, **1987**, *326*, 450.
(4) Matthews, J. W.; Blakeslee, A. E.; Mader, S. *Thin Solid Films* **1976**, *33*, 253. Osbourn, G. C. *J. Vac. Sci. Techol.* **1982**, *21*, 469.

0002-7863/88/1510-7630$01.50/0